

# Compton Spectroscopy and Chemical Bonding

By Abhay Shukla<sup>1,\*</sup>, Bernardo Barbiellini<sup>2</sup>, Thomas Buslaps<sup>1</sup> and Pekka Suortti<sup>3</sup>

<sup>1</sup> European Synchrotron Radiation Facility, BP 220, F-38043 Grenoble, France

<sup>2</sup> Physics Department, Northeastern University, Boston, Ma 02115-5000, U.S.A

<sup>3</sup> Department of Physics, PB 9, FIN-00014, University of Helsinki, Finland

*Dedicated to Prof. Dr. Dr. h.c. Wolf Weyrich  
on the occasion of his 60th birthday*

(Received May 18, 2001; accepted June 5, 2001)

## *Momentum Density / Chemical Bonding / Compton Profile*

In this article we show with the help of two examples how Compton spectroscopy may be used to study the effect of chemical bonding in materials as diverse as a molecular crystal and a high temperature superconductor. Compton spectroscopy has a long history as an investigative method in condensed matter physics and in fact the realisation that the Compton profile is sensitive to the effects of chemical bonding dates back at least fifty years. In the seventies, through the efforts of Weyrich [1] and others [2,3], practical applications of this realisation were first achieved. We argue that such studies are more and more relevant thanks to the availability of synchrotron radiation and efficient computational tools.

## 1. Introduction

Compton scattering, or inelastic scattering with very high momentum and energy transfer is a probe of the ground state, one-electron properties of the system [4]. The measured one dimensional quantity  $J(p_z)$  is a projection of the three dimensional electronic momentum density  $\rho(\mathbf{p})$  onto the scattering vector (parallel to  $\mathbf{p}_z$ ):

$$J(p_z) = \int_{-\infty}^{\infty} \rho(\mathbf{p}) dp_x dp_y. \quad (1)$$

Experimental Compton profiles used in this article were measured using the high-resolution scanning spectrometer at ID15B at the ESRF[5].

---

\* E-mail: shukla@esrf.fr

## 2. Ice crystal

Our first example is related to the measurement of Compton Profile anisotropy in the ice Ih crystal. Many earlier works [6, 7] measured the Compton profile in liquid water and were able to isolate the effect of an antibonding contribution. In our recent x-ray Compton scattering experiment in ice Ih [8] Compton profiles were measured along the  $c$  direction and nearly along the  $a$  direction (6 degrees from  $a$  in the  $a$ - $b$  plane). We refer to the corresponding anisotropy as the  $c$ - $a/b$  anisotropy, since the shape of the anisotropy remains the same for all directions in the  $a$ - $b$  plane. It was shown that this anisotropy ( $c$ - $a/b$ ) of the Compton profile has a characteristic signature ascribed to the quantum nature of hydrogen bonding by comparison with theoretical calculations for an ice crystal and a monomer. This behaviour was described as partial covalency.

In an article based on calculations for the  $H_2O$  dimer Ghanty *et al.* [9] stated that experimental Compton anisotropies ( $c$ - $a/b$ ) in ice Ih measured in [8] are a result of the repulsive exchange interaction due to the Pauli exclusion principle which forbids overlap of filled orbitals in the crystal.

Working with their single determinantal wave functions they showed that the dominant structure in the Compton profile anisotropy for an oriented dimer is already there in the calculation for the anti-symmetrized unrelaxed dimer, which has a net repulsive energy at an O...H distance of 2.75 Å. Therefore, they concluded that the observed interference phenomenon arises from an anti-bonding interaction.

The energy partitioning for the hydrogen bond was first considered by Coulson and Danielson in 1954 [10]. These authors considered a minimum (non-orthogonal) basis set description and showed that the lone pair orbital of the oxygen mixes with an antibonding orbital OH. Ghanty *et al.* [9] have argued that such mixing is also produced by orthogonalizing the minimum basis set. Our motivation here is to investigate to what extent effects due to relaxation beyond the dominant effect ascribed to an anti-bonding interaction may be observed. To do this we use our experimental anisotropy, the theoretical curves in [9] for the unrelaxed, anti-symmetrized dimer (orth.) and the fully relaxed dimer (DFT) as well as the DFT calculation in [8] (DFT-GGA). Here we are only concerned with the shape of the anisotropy and the theoretical amplitudes have been normalised to the first peak in the experimental anisotropy. Fig. 1 compares data with the three theoretical approaches and though the general shape is similar it is clear that differences are significant. Features absent in the unrelaxed dimer appear in the relaxed dimer and become more pronounced in the theory for the crystal and in the data, in particular the peak at 0.3 a.u. The period of the oscillations in the calculations for the dimer is also somewhat different, especially at small  $p$ , which implies that longer range interactions are not faithfully reproduced in real space for the dimer. These differences are well above statistical error and merit further analysis.

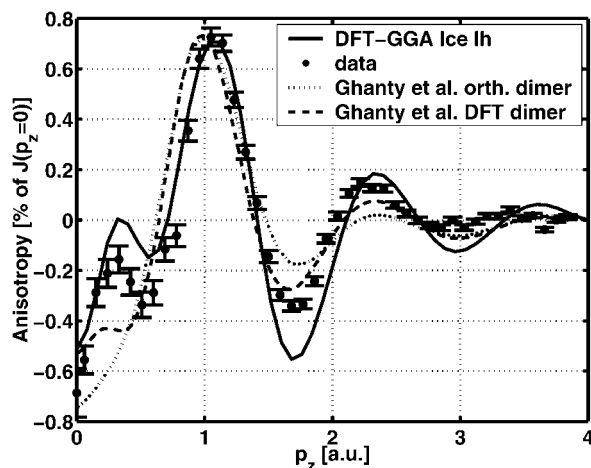


**Fig. 1.** Compton anisotropies in Ice. ( $J_c - J_{a-b}$ ), plotted as % of the peak intensity of the Compton profile for the data. The theoretical curves have been scaled to the amplitude of the first peak in the data. Solid circles: data, solid line: DFT calculation from [8], dotted line: orthogonalised, unrelaxed dimer calculation from [9], dashed line: fully relaxed dimer calculation from [9].

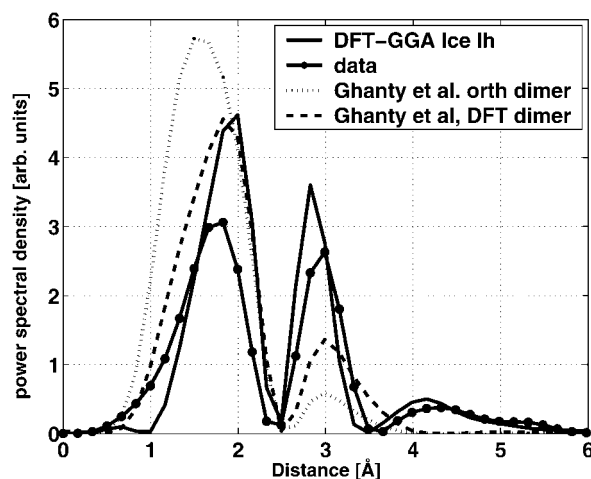


**Fig. 2.** Power density of the Compton anisotropies in Fig. 1. Connected solid circles: data, solid line: DFT calculation from [8], dotted line: orthogonalised, unrelaxed dimer calculation from [9], dashed line: fully relaxed dimer calculation from [9].

As we have pointed out in [8] the power density of the anisotropy (the square of the anisotropic  $B(r)$  function) separates in real space the different length scales contributing to the oscillations in the anisotropy in momentum

space. In comparing these power densities in Fig. 2 for the different calculations and the data, the above mentioned trend becomes clear. Because of the scaling of amplitudes involved, only the relative intensities of peaks in the same spectrum may be compared. In this representation the unrelaxed dimer compares unfavorably with the data. The first peak ( $\sim 1.5 \text{ \AA}$ ) is broad and shifted to a lower value. The second peak ( $\sim 2.8 \text{ \AA}$ ) is much smaller. In the relaxed dimer the situation improves with the first peak narrowing and shifting to a higher value and the second peak becoming stronger. In our calculation for the crystal, both peaks are of comparable amplitude and interestingly an additional peak corresponding to distances greater than  $4 \text{ \AA}$ , appears, as in the data. The inescapable conclusion is that these effects are due to relaxation and that information on effects (charge transfer and polarization) more subtle than the dominant exchange interaction can be obtained. This makes Compton spectroscopy a unique tool for the study of weak inter-molecular interactions, a fact already noted by Bräuchler *et al.* [11]

### 3. High $T_c$ superconductors

Our second example [12] concerns a high  $T_c$  superconductor,  $\text{YBa}_2\text{Cu}_3\text{O}_{7-\delta}$ . Our aim here is not to investigate Fermi surface properties, a task which is not feasible given the complexity of the system, but to see if Compton spectroscopy can be used to understand the insulating behaviour of  $\text{PrBa}_2\text{Cu}_3\text{O}_{7-\delta}$ , the compound where Y is replaced with Pr. It should be remarked that the substitution of Y with other rare-earths does not destroy superconducting properties.

We now discuss the anisotropy of the Compton profiles, that is, the difference between Compton profiles measured in two crystallographic directions ( $J_{[100/010]} - J_{[110]}$ ). The anisotropy has the advantage of getting rid of the isotropic contribution of the core electrons as well as residual background. Since both measured directions are in the a-b plane, the structure in the anisotropy originates essentially in this plane, but includes contributions from all entities of the unit cell, the Cu-O chains, the Ba-O and Y/Pr planes as well as the Cu-O layers. However from earlier momentum density measurements [13] as well as other experiments [14, 15] it has been established that the Cu-O chains are identical in both materials, being locally metallic with a corresponding Fermi surface (even in  $\text{PrBa}_2\text{Cu}_3\text{O}_{7-\delta}$ ). It is thus safe to say that any differences between the two originate in the remaining entities, the Cu-O layers or the Ba-O and Y/Pr planes.

For comparison with experiment we have computed theoretical Compton profiles based on LDA band-structure with the FLAPW method [16] (for  $\text{YBa}_2\text{Cu}_3\text{O}_{7-\delta}$ ) and the LMTO method [17] (for  $\text{PrBa}_2\text{Cu}_3\text{O}_{7-\delta}$ ). The calculation for  $\text{PrBa}_2\text{Cu}_3\text{O}_{7-\delta}$  shows that the band structure is qualitatively similar to that of  $\text{YBa}_2\text{Cu}_3\text{O}_{7-\delta}$ . The LMTO method was chosen for the PrBCO calculation as it is more flexible for the purposes of a model calculation used later

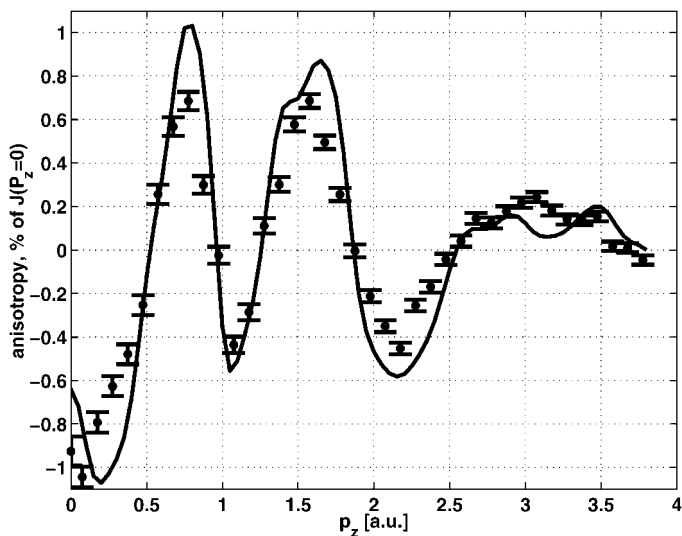


**Fig. 3.** Anisotropy ( $J_{[100/010]} - J_{[001]}$ ) in the electron momentum density of  $\text{YBa}_2\text{Cu}_3\text{O}_{7-\delta}$ . Note the good overall agreement between the experiment and the LDA calculation (solid line), scaled to the experimental variation.

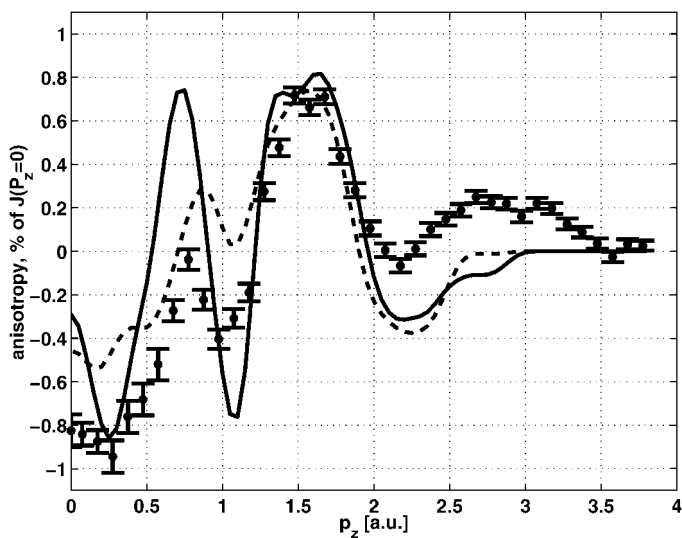


**Fig. 4.** Anisotropy ( $J_{[100/010]} - J_{[001]}$ ) in the electron momentum density of  $\text{PrBa}_2\text{Cu}_3\text{O}_{7-\delta}$ . The calculated LDA result (solid line), scaled to the variation in experiment, is very similar to that for  $\text{YBa}_2\text{Cu}_3\text{O}_{7-\delta}$  (Fig. 1) implying that Pr-O hybridization has minimal influence on electronic structure. The experiment differs remarkably, the first peak in the anisotropy being strongly suppressed with respect to  $\text{YBa}_2\text{Cu}_3\text{O}_{7-\delta}$ . A simple theoretical model assuming disorder in the Ba-O and Pr planes (dashed line) shows similar behaviour.

in the text. In Ref. [12] the PrBCO anisotropy is estimated with the YBCO FLAPW anisotropy as a starting point and the differences between these two approaches (FLAPW and LMTO) is minor in this case.

The anisotropy is shown as a percentage of the peak value of the Compton profile. The amplitude of the anisotropy in the theory is about 40% larger than in the experiment. In the figures shown the theoretical anisotropy is scaled to the experimental one by a factor of 1.4 to ease comparison. Fig. 3 shows the measured and calculated (solid line) anisotropy for  $\text{YBa}_2\text{Cu}_3\text{O}_{7-\delta}$ . The two are remarkably alike, showing that the overall description of the electronic structure is satisfactory. Fig. 4 shows the measured and calculated (solid line) anisotropy for  $\text{PrBa}_2\text{Cu}_3\text{O}_{7-\delta}$ . Firstly, the theoretical curve is essentially the same as for  $\text{YBa}_2\text{Cu}_3\text{O}_{7-\delta}$ : in-plane properties change little on replacing Y with Pr in the calculation. The experimental curve however is very different, with a much smaller amplitude for the first peak in the anisotropy. Differences at higher momentum ( $\geq 2.5$  a.u.) stem from a cutoff in the LMTO calculation.

There is substantial evidence that even in globally stoichiometric samples of  $\text{PrBa}_2\text{Cu}_3\text{O}_{7-\delta}$  substitution disorder concerning the Pr and Ba sites (spinodal decomposition for example) exists locally [19, 20], especially if growth is followed by slow-cooling. Such disorder, due to the large size of Pr ions has also been observed in the case of similar sized Nd [20] and La [19] ions. The amount of this substitution has been estimated to be a maximum of about 8%. If such disorder were present, the contribution of the Pr and Ba-O planes to the total anisotropy would be strongly suppressed due to the absence of long-range order in these planes. For qualitative comparison we have accounted for this using a simple model where the Pr and Ba-O planes do not contribute to the total anisotropy. We assume that the corresponding contributions from the atomic spheres (used in the LMTO method to partition the space) are purely spherical since the phases, producing the anisotropies, interfere destructively in presence of disorder. Thus only the anisotropy coming from the contribution of the Cu-O planes is considered. The resulting theoretical curve (dashed line), shown in the same figure mimics the strong suppression of the first peak in the anisotropy. Given these facts we argue that this disorder is in fact at the basis of the lack of superconductivity and metallicity in  $\text{PrBa}_2\text{Cu}_3\text{O}_{7-\delta}$ . Pr on the Ba site is probably in a 4+ oxidation state, which while maintaining the carrier concentration in the Cu-O chains, inhibits hole-doping in the Cu-O planes, preventing metallic behaviour. Strong support for this interpretation was provided by the fact that by using a combined strategy to minimize substitution disorder [20] and avoid tetravalent  $\text{Pr}_{\text{Ba}}$ , it was possible to obtain small flux-grown crystallites of  $\text{PrBa}_2\text{Cu}_3\text{O}_{7-\delta}$  with a  $T_c$  of 90 K and a bulk Meissner effect.

We hope to have shown with these two examples that the sensitivity of the Compton profile to aspects of chemical bonding can make it a useful tool in chemical applications. This will need a simultaneous and systematic effort both on the experimental and the theoretical side but holds considerable promise in

the field of better understanding of weak effects like inter-molecular interactions where traditional charge-density methods become insensitive.

### Acknowledgement

We acknowledge E. Isaacs and P. Platzman who initiated the ice measurement and Andreas Erb and Alfred Manuel who collaborated on the  $\text{PrBa}_2\text{Cu}_3\text{O}_{7-\delta}$  experiment. B. B. is supported by the U.S. Department of Energy under Contract No. W-31-109-ENG-38 and this work benefitted from the allocation of supercomputer time at the Northeastern University Advanced Scientific Computation Center (NU-ASCC).

### References

1. W. Weyrich, P. Pattison and B. Williams, *Chem. Phys.* **41** (1979) 271.
2. P. Pattison, W. Weyrich and B. Williams, *Solid State Commun.* **21** (1977) 967.
3. P. Pattison, N. K. Hansen and J. R. Schneider, *Chem. Phys.* **51** (1981) 231.
4. *Compton Scattering*; B. G. Williams, Ed., McGraw-Hill, New York (1977).
5. P. Suortti, T. Buslaps, P. Fajardo, V. Honkimäki, M. Kretzschmer, U. Lienert, J. E. McCarthy, M. Renier, A. Shukla, Th. Tschentscher and T. Mienander, *J. Synchrotron Rad.* **6** (1999) 69.
6. S. Manninen, T. Paakkari and V. Halonen, *Chem. Phys. Lett.* **46** (1977) 62.
7. A. Seth and E. J. Baerends, *Chem. Phys. Lett.* **52** (1977) 248.
8. E. D. Isaacs, A. Shukla, P. M. Platzman, D. R. Hamann, B. Barbiellini, and C. Tulk, *Phys. Rev. Lett.* **82** (1999) 600.
9. T. K. Ghanty, V. N. Staroverov, P. R. Koren and E. R. Davidson, *J. Am. Chem. Soc.* **122** (2000) 1210.
10. C. A. Coulson and U. Danielsson, *Arkiv Fysik* **8** (1954) 245.
11. M. Bräuchler, S. Lunell, I. Olvsson and W. Weyrich, *Int. J. Quantum Chem.* **35** (1989) 895.
12. A. Shukla, B. Barbiellini, A. Erb, A. Manuel, T. Buslaps, V. Honkimäki and P. Suortti, *Phys. Rev. B* **59** (1999) 12127.
13. L. Hoffmann, A. A. Manuel, M. Peter, E. Walker, M. Gauthier, A. Shukla, B. Barbiellini, S. Massidda, Gh. Adam, S. Adam, W. N. Hardy and R. Liang, *Phys. Rev. Lett.* **71** (1993) 4047.
14. A. Shukla, L. Hoffmann, A. A. Manuel, E. Walker, B. Barbiellini and M. Peter, *Phys. Rev. B* **51** (1995) 6028.
15. K. Takenaka, Y. Imanaka, K. Tamamsaku, T. Ito and S. Uchida, *Phys. Rev. Lett.* **46** (1992) 5833.
16. S. Massidda, J. Yu, A. J. Freeman and D. D. Koelling, *Phys. Lett. A* **122** (1987) 198.
17. B. Barbiellini, P. Genoud, J. Y. Henry, L. Hoffmann, T. Jarlborg, A. A. Manuel, S. Massidda, M. Peter, W. Sadowski, H. J. Scheel, A. Shukla, A. K. Singh and E. Walker, *Phys. Rev. B* **43** (1991) 7810.
18. M. P. Nutley, A. T. Boothroyd and G. J. McIntyre, *J. Magn. Magn. Mater.* **104–107** (1992) 623.
19. H. A. Blackstead, J. D. Dow, D. B. Chisey, J. S. Horwitz, M. A. Black, P. J. McGinn, A. E. Klunzinger and D. B. Pulling, *Phys. Rev. B* **54** (1996) 6122.
20. A. Erb, E. Walker and R. Flükiger, *Physica C* **9** (1996) 258; A. Erb, E. Walker, J.-Y. Genoud and R. Flükiger, *Physica C* **89** (1997) 82.